Astro. Lett. and Communications, Vol. 37, pp. 85–107
Reprints available directly from the publisher
Photocopying permitted by license only

ZEEMAN SPLITTING OPPORTUNITIES AND TECHNIQUES AT ARECIBO

CARL HEILES

Astronomy Department, University of California, Berkeley CA 94720 USA

We begin with a discussion of the instrumental errors for measurements of emission lines caused by polarized sidelobes. Previously obtained results are generally reliable. Arecibo should be an excellent telescope for such studies.We then discuss a number of Zeeman-splitting observations for which Arecibo should eminently suitable. We consider mainly the 21-cm emission line in the Milky Way and in nearby galaxies, but also consider recombination lines, excited CH, and highly redshifted 21-cm absorption lines.

Keywords: Galaxies: magnetic fields; ISM: magnetic fields; techniques: polarimetric

1. FUNDAMENTALS

Interstellar magnetic fields are very weak and in all cases except masers produce Zeeman splitting that is much smaller than the line width ($\Delta\nu_Z \ll \delta\nu$). This makes Zeeman splitting observations sensitivity limited. Accordingly, the only hope of detecting the splitting is with an atom or molecule whose splitting is "large", which means that the molecule must have a large magnetic moment μ and Landé factor g. The magnetic moment is "large" ($\sim$ the Bohr magneton $e\bar{h}/2m_e c$) for species with electronic angular momentum and otherwise thousands of times smaller ($\sim$ the nuclear magneton $e\bar{h}/2m_n c$). Thus, only species with electronic angular momentum are useful for Zeeman splitting experiments. Heiles *et al.* (1993) describe the details and provide a list of atoms and molecules having electronic angular momentum. Suitable species for Arecibo (with line frequencies < 12 GHz) include HI, Radio Recombination Lines, OH, CH, C_4H and C_2S. Examining

different species is useful because they sample different regimes of density; one usually expects the magnetic field strength to increase with density.

For the case $\Delta\nu_Z \ll \delta\nu$, Zeeman splitting is detectable in the Stokes V spectrum, which is the difference between the two circular polarizations. The V spectrum has the shape of the first derivative of the line profile (the Stokes I spectrum) with an amplitude $\alpha\ B_\parallel$, where $B_\parallel$ is the line-of-sight component of the field. The Zeeman effect exhibits itself only in terms of this frequency difference and intensity differences between the two circular polarizations are irrelevant. This is fortunate, because it is difficult in practice to construct a polarimeter in which the gains for the two circular polarizations are equal to the required accuracy. Accordingly, one usually performs a two-term least-squares fit of the V spectrum to the I spectrum in which one term represents the frequency difference and the other the amplitude difference; Zeeman splitting depends only on the former (see Troland and Heiles, 1982; TH).

2. INSTRUMENTAL EFFECTS IN EMISSION LINE MEASUREMENTS

Here we concentrate on the 21-cm line, for which instrumental effects are probably the most severe because it is so widely distributed. The interstellar magnetic field in HI regions can be measured from the Zeeman splitting of the 21-cm line as seen in both absorption and emission. Emission measurements have the great advantage that one can look anywhere, so that the field in interesting regions can be measured and mapped. However, emission measurements are prone to instrumental error from polarized sidelobes.

2.1. Description of Polarized Sidelobes in Terms of a Taylor Series

Observing Zeeman splitting amounts to observing the sky with a "circularly-polarized beam", i.e., the Stokes V-beam. In practice, this V beam is not a "clean beam" because it has sidelobes. TH used both their empirical investigations of the Hat Creek (HCRO) 85-foot

telescope and theoretical investigations published by others to classify these V sidelobes three primary ways:

(1) *Beam squint, in which the two circular polarizations point in different directions with a separation and direction* $\vec{\Psi}_{BS}$* . This produces a "two-lobed" V beam, in which the lobes are located on opposite sides of beam center, have opposite signs with amplitude $\propto \Psi_{BS}$, and are separated by about one half-power beamwidth (HPBW). This two-lobed structure responds to the first derivative of the 21-cm line on the sky. If the line has a velocity gradient $\vec{\nabla}_v$, then this structure produces a velocity difference $\Delta v = \vec{\nabla}_v \cdot \vec{\Psi}_{BS}$ between the two circular polarizations. This directly mimics the observational signature of Zeeman splitting.

(2) *The presence of residual linear polarization in what should be pure circular polarization.* In other words, the observations are made with slight elliptical polarization instead of pure circular polarization. This produces a "four-lobed" V beam, in which two lobes on opposite sides of beam center have the same sign and two lobes rotated 90° in position angle have the opposite sign. This four-lobed structure responds to the second derivative of the 21-cm line on the sky. As explained by TH, it is easy to measure this astronomically and use the result to adjust the polarimeter for pure circular polarization. In practice with the HCRO telescope, we found no evidence for any significant contribution from this effect, and this is illustrated by the following: Heiles (1989, §IIa) unknowingly observed many positions with a poorly-adjusted polarimeter and, after discovering the maladjustment and correcting it, reobserved these positions. He found no discernible difference.

(3) *Instrumental polarization outside the main beam and at large angles from beam center.* This includes sidelobe structure at all scales larger than the main telescope beam. The total power in these "distant sidelobes" is nontrivial: they are weak, but they cover a very large solid angle; furthermore, they tend to be highly elliptically polarized. These "distant sidelobes" are a result of

*In this paper, vector quantities on the sky are indicated with the arrow and those quantities without the arrow are the magnitudes of the vectors.

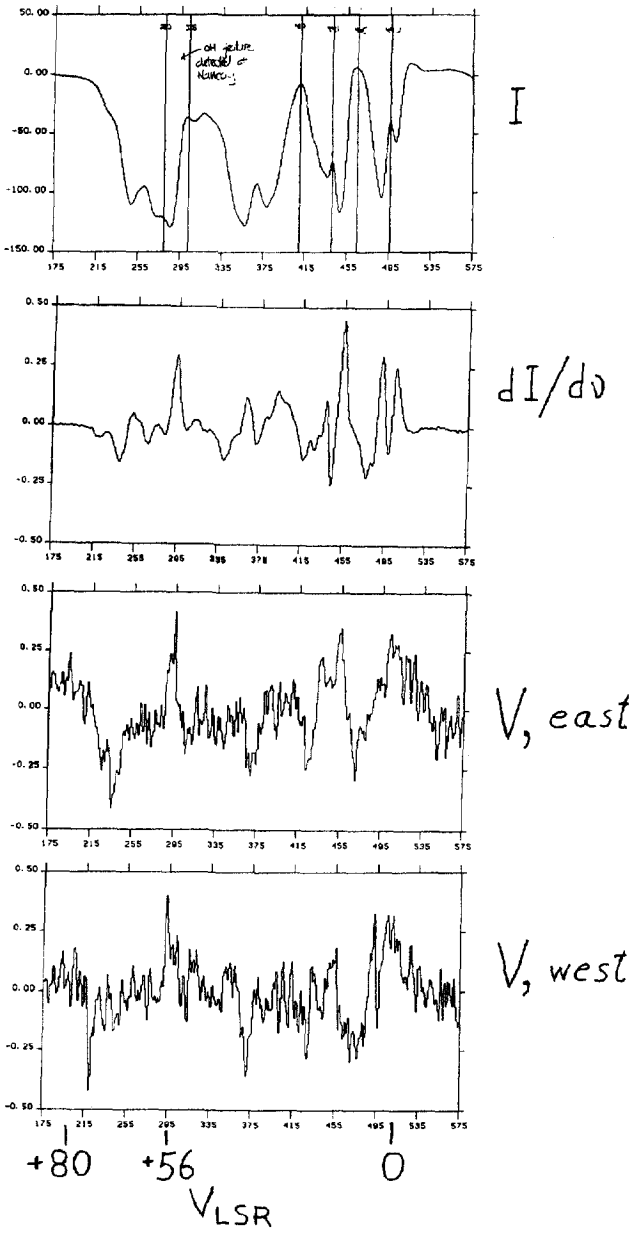

FIGURE 1 Observations of the 21-cm line in absorption against W49 made at Arecibo in 1987 by Troland and the author. The vertical scale is antenna temperature in Kelvins; the horizontal scale is channel number, with the LSR velocity scale inserted by hand at the bottom. Top panel: the Stokes I spectrum; next, the frequency derivative of the I spectrum scaled to $B_{\|} = 10\ \mu G$; next, the observed V spectrum at eastern hour angles; bottom, the observed V spectrum at western hour angles.

telescope surface roughness and the feed leg structure. TH found that within 4° of beam center the polarized sidelobe structure is "jumbled and irregular". They did not explicitly state the fact this structure is so weak that its existence is barely measurable. To see it TH tried using Cas A, the strongest "point-source" continuum source availble; Cas A was too weak to reliably map this structure. TH also tried using the Sun to map it, but the Sun is not sufficiently a point source to probe this structure, whose angular scale is comparable to the HPBW. TH were successful in using the Sun to probe the feed leg rings, which have much larger angular scale (see their Fig. 1).TH found that these sidelobes, even with their larger total power, are unimportant in practice because they produce broad, weak features in the V spectrum that are easy to distinguish from the narrower features produced by HI clouds.

This threefold classification is equivalent to a two-dimensional Taylor expansion of the polarized sidelobe structure. TH found this to be an excellent description of the actual polarized sidelobes for the HCRO telescope. This is reflected in the fact that TH made complete maps of the sidelobes only near the beginning of their efforts, in the late 1970's; it rapidly became clear that it was much easier and more efficient to parameterize the maps with the above classification. In fact, no complete maps of the V beam remain available for the HCRO telescope.

The appropriateness of this threefold classification also applies to the Green Bank 140-foot telescope, as can be seen in the maps of its V beam presented by Verschuur (1969, 1989). Verschuur's (1969) Figure 2 presents the V beam pattern for the 140-foot telescope as it was in the late 1960's. At that time, it was very well described by beam squint with a peak-to-peak amplitude of about 1.4%; this corresponds to a beam squint $\Psi_{BS} \approx 7'$. Our maps of the complete polarized sidelobe structure of the HCRO telescope always produced similar results, although with much smaller beam squint. Verschuur's (1989) Figure 1 presents the 140-foot polarized beam structure as it was in the late 1980's, and shows a drastic difference: the newer map shows primarily the four-lobed pattern of our category (2) with little beam squint. The 1960's version of the beam pattern made the 140-foot telescope unsuitable for Zeeman-splitting measurements of HI in emission because the beam squint contribution to instrumental error would

have been excessive. However, the 1980's version, with its small beam squint but higher second-derivative component, was satisfactory – as shown by the fact that Verschuur reobserved four positions that had previously been observed with the HCRO telescope and found excellent agreement in three, as discussed in some detail by Heiles (1990).

2.2. How to Estimate the Instrumental Contribution of Beam Squint

Beam squint, being the first term in the two-dimensional Taylor series that describes the polarized beam structure, directly samples the first derivative of the HI line on the sky. In general, this first derivative contains a velocity derivative. Thus, at some level, the beam squint must produce an instrumental contribution to the V spectrum that mimics that from Zeeman splitting. It is crucial to determine the level of this contribution and to either subtract it out or reduce it to the level of unimportance.

It is straightforward to estimate the beam squint instrumental effect. If the line has a velocity gradient $\vec{\nabla}_v$, then this structure produces a velocity difference $\Delta v = \vec{\nabla}_v \cdot \vec{\Psi}_{BS}$ between the two circular polarizations. Thus we must know both the beam squint and the velocity gradient.

2.2.1. The Velocity Gradient

First we consider the velocity gradient. The *total* velocity gradient is what contributes to the instrumental error. There are two components to the gradient. One (the "LSR") involves the motion of gas with respect to the Sun in the frame of the local standard of rest; the second (the "heliocentric") involves the Earth's motion in its orbit around the Sun with respect to the gas.

If one directly measures the velocity gradient at the telescope, one might follow our procedure and make a five-point map. For these five points one should always use the local oscillator frequency that is appropriate to the central position, *without* using different Doppler

corrections for the different positions; this properly measures the total velocity gradient for the particular time of year of the measurement.

Alternatively, one can evaluate the velocity gradient from a catalog of HI profiles; with this procedure, the LSR contribution is accounted for because velocities are always given with respect to the local standard of rest. The statistics of the LSR contribution are given by Heiles (1996), who finds $\langle \nabla v_{LSR} \rangle = 0.73$ km s^{-1}deg^{-1}.

However, the heliocentric contribution, is not accounted for; obviously, the result depends on the time of year. The Earth's orbital velocity is about 30 km s^{-1}, and the maximum derivative is 0.5 km s^{-1}deg^{-1}. This must be vectorially added to the LSR gradient; because there is no correlation between the two directions, we combine the heliocentric rms value of 0.42 km s^{-1}deg^{-1}in quadrature with $\langle \nabla v_{LSR} \rangle$ to obtain $\langle \nabla v \rangle = 0.84$ km s^{-1}deg^{-1}for the representative total velocity gradient. The beam squint interacts with the total velocity gradient and, because there is no correlation between the two directions, the beam squint will typically see only $\langle v \rangle / \sqrt{2}$. Thus, we adopt $\nabla v = 0.6$ km s^{-1}deg^{-1}as the typical total velocity gradient seen by the beam squint.

With $\nabla v = 0.6$ km s^{-1} deg^{-1}, the typical instrumental contribution to beam squint is $B_{BS} = 0.28\ \Psi_{BS}\ \mu G$, where Ψ_{BS} is in arcseconds. Typically, a beam squint of 3 arcseconds produces $B_{BS} < 1\ \mu G$, which is usually significantly (but not negligibly) smaller than the field strengths that are being measured. One caveat: Arecibo, with its 100-times smaller beam area than the HCRO telescope, may see different statistics for the velocity gradient!

2.2.2. The Beam Squint

It is straightforward to measure this on a small continuum source. The most important contributing factor to beam squint is the feed not pointing directly at the vertex of a paraboloid, and one can minimize beam squint by changing this angle. This also means factors such as gravitational deformation cause a positional dependence of beam squint. A full understanding of beam squint requires measuring its positional dependence. This positional dependence is one important reason for parameterizing the polarized beam as a Taylor series, because the positional dependence of the coefficients can be treated in a straightforward fashion.

We can quote some representative values for beam squint; for the NRAO telescope in the late 1960's, $\Psi_{BS} \sim 7''$ (Verschuur 1969); for the HCRO telescope at the NCP, $\Psi_{BS} \sim 3''$ (Heiles, 1996); for the HCRO telescope typically, $\Psi_{BS} \leq 3''$ and typically $\sim 1''$ (Heiles, 1996); for Arecibo, the predicted $\Psi_{BS} \leq 0.3''$.

2.3. How to Empirically Measure the Instrumental Contribution of Beam Squint

This *empirical* technique employs rotation of the beam pattern with respect to the sky. For an alt-az telescope, this rotation occurs naturally as a position is tracked. However, with an equatorial telescope, the beam pattern remains fixed on the sky during tracking (apart from changes produced by gravitational deflection and the like). Nevertheless, there is one position for which rotation can be made to occur: the Celestial Pole. We describe this as an example of the technique. The North Celestial Pole [the NCP: $(\ell, b) \approx (123°, 27°)$] contains a bright HI filament and is part of a region that is well-studied in CO and 100 μm emission (e.g., Heithausen and Thaddeus, 1990). Heiles (1989) has measured $B_{\|}$ with HI Zeeman splitting in emission for many positions in the filament; typically, $B_{\|} \sim +10\ \mu G$.

Heiles (1996) describes the details and results of this technique when applied to the Hat Creek telescope and the NCP. He divides the data into 12 time ("Right Ascension" or RA) bins and measures the magnetic field strength $B_{\|}$ separately and independently for each. He then Fourier analyzes the 12 results.

Consider first Error (1), with the beam squint's two-lobed pattern. Suppose that at a particular RA_+ the pattern is "lined up" with the direction of the local 21-cm line gradient; the subscript + means that at this RA, the beam squint error is maximum and is positive in sign. 12 hours later the pattern will have rotated 180° on the sky, the positive and negative lobes will have interchanged, and the beam squint error will be the same in magnitude, but negative in sign. Thus, the instrumental error produced by the two-lobed pattern produces a Fourier component with one cycle per 24 hours (the "first Fourier component") whose amplitude is equal to the instrumental error from this effect.

The situation is similar for Error (2): Suppose that at RA_+ it is lined up with the local second derivative. 6 hours later it will have rotated 90° on the sky, the positive and negative lobes will have interchanged, and the instrumental error will be the same in magnitude, but negative in sign. Thus, the instrumental error produced by the four-lobed pattern produces a Fourier component with two cycles per 24 hours (the "second Fourier component") whose amplitude is equal to the instrumental error from this effect.

For the average of all RA's Heiles (1996) found the V spectrum to be an excellent fit to the derivative of the I spectrum, with $B_{\|} = 8.9 \pm 0.3$ μG; this is in excellent agreement with the nearby measurements of Heiles (1989). He also found a systematic variation of $B_{\|}$ with RA from ~ 7 to 12 μG, indicating the contribution of instrumental errors. The amplitude of the first Fourier component ~ 2.0 μG and of the second ~ 0.58 μG. The first Fourier component is significantly higher than the others, while the second is comparable to them and is probably not significant with respect to noise.

These data show that the dominant instrumental error arises from beam squint and, at the NCP, has a maximum value of 2.0 μG. The typical value, i.e., the average error that would be obtained with an arbitrary orientation of the beam squint with respect to the velocity gradient at the NCP, is $\sqrt{2}$ times smaller, 1.4 μG. This is safely smaller than the field strengths in the vicinity.

2.4. Verschuur's Recent Claims

Measurements of Zeeman splitting of HI emission lines have been made by TH, Heiles and his collaborators, and Verschuur. Until recently, the agreement has been quite good. Verschuur (1989) reobserved four positions that had previously been observed with the HCRO telescope and found excellent agreement in three, as discussed in some detail by Heiles (1990).

However, more recently Verschuur (1993) has claimed that "... claims of Zeeman effect detections in HI emission features ... based on observations made with presently available single-dish radio telescope cannot be regarded as reliable." At the time of his paper, the HCRO telescope had already been destroyed, but he meant his claim to apply

to that telescope as well as other telescopes that still exist. We believe his claim to be incorrect. His claim is based on his estimates of the instrumental effects, which in turn are based solely on measurement of the velocity gradient of the HI line (Verschuur, 1995a, 1995b). In particular, his estimates of the instrumental effects are not based at all on the properties of the polarized beam.

Verschuur's (1995b) procedure for correcting an observed V profile for the beam squint contribution and deriving the Zeeman splitting consists of 6 steps:

(1) Observe a V and I spectrum at the central position P; denote these $V_{obs}(v)$ and $I_{obs}(v)$.
(2) Make an 8-point map of I spectra around P. Each map position is displaced from P by 15 arcminutes; in position angle the 8 points are equally spaced (45°), with the displacements of 4 points towards the cardinal directions in equatorial coordinates.
(3) Find the pair of profiles whose difference spectrum $\Delta(v)$ is strongest and mimics the shape of $V_{obs}(v)$
(4) Find the coefficient R that scales the Δ spectrum to the V_{obs} spectrum, i.e., the best fit for $R\Delta(v) = V_{obs}(v)$
(5) Produce the "corrected" V spectrum $V_{corr}(v) = V_{obs}(v) - R\Delta(v)$.
(6) Derive the Zeeman splitting from V_{corr}.

The fatal flaw is that R, which represents the beam squint, is not measured directly for the telescope, Rather, it is given the particular value that minimizes the observed V spectrum $V_{obs}(v)$.

As explained above in §2.1, the beam squint samples the first derivative of the 21-cm line on the sky and must contain a velocity gradient at some level. Steps 2 and 3 of the above procedure measure the velocity gradient. Step 4 fits this velocity gradient to the observed V spectrum and derives the coefficient R. In essence, R is equal to the projection of the *assumed* beam squint along the velocity gradient in units of 30 arcmin. Then, no matter how large R is, it is used to subtract away the scaled Δ profile from the observed V spectrum.

But the amplitude of the beam squint can be independently measured for a telescope. The proper procedure would be to measure the beam squint and velocity gradient, multiply the two vectorially, and subtract the result from the observed V spectrum.

Consider one particular entry in Verschuur's (1995b) Table II as an example: NCP-Shell.4. For this position he obtains $R = 0.0052$ (In Tab. II, R is given in column 5.). This corresponds to a beam squint of 30 arcmin $\times$ 0.0052 = 9.4 arcsec. This is far higher than the beam squint of the Hat Creek telescope near the North Pole, which Heiles (1996) estimates as 3 arcsec. Verschuur uses this value of R to subtract away a velocity derivative from the V_{obs} profile that amounts to 10.8 μG, obtaining a "corrected" field stength 2.1 $\pm$ 1.0 μG. In doing this he has removed the contribution to V_{obs} that arises from the magnetic field – he has removed the "signal".

The data in Verschuur's (1995a, 1995b) papers could be reanalyzed taking account of the fact that the beam squint of the 140 foot telescope is limited to some maximum value. Unfortunately, this is not discussed by Verschuur, but judging from his earlier paper in this field (Verschuur, 1989) the upper limit on 140-foot beam squint is probably $\sim$ 3 arcsec, which corresponds to R = 0.0017 (0.17%). Many entries in Verschuur's table have $R >$ 0.0017 and these probably represent real measurements of Zeeman splitting.

2.5. Arecibo's Capabilities: Observational Examples

Some of us (Goodman *et al.*, 1989) have used Arecibo for Zeeman splitting measurements of the 18-cm OH lines, obtaining a successful measurement in the dark cloud Barnard 1 together with several other nondetections. Others of us have also used Arecibo to make unpublished observations of the 21-cm line, which were all unsuccessful because of uncertainties of the instrumental effects. We recount two examples here to illustrate these difficulties.

The first example is our observations of HI absorption against the strong continuum source W49. This source is located on the Galactic equator, 12.5 kpc distant, and as a result has the complicated HI absorption spectrum shown at the top of Figure 1. As explained above in §1, the Zeeman effect exhibits itself in the Stokes V spectrum with a shape of the derivative of the I spectrum; just below the top panel we show the Stokes V spectrum that would be observed for a field $B_{\|} = 10$ μG. Below that we show two observed V spectra, one for east hour angles and one for west hour angles. The fact that these differ must be

a result of instrumental effects. The differences are at the $\sim$ 10 μG level. Thus, Zeeman "detections" at this level are not reliable. At V_{lsr} $\sim$ 56 km s^{-1} we see a positive-going feature that is identical in the two V spectra. This does not mean that it is real! Nevertheless, it is intriguing that this is the velocity at which Zeeman splitting in the 18-cm OH lines is also seen (Crutcher, Kazès and Troland, 1987); the sign of the HI field, if it is real, is positive – the same as the OH field – and the magnitude about half that of the OH field.

This example on W49 shows that Arecibo, with its line feeds, was almost good enough to see fields at the 10 μG level. We did not apply any corrections for beam squint or other polarized sidelobe structure to these data; such corrections should reduce the instrumental contributions by something approaching an order of magnitude, which would have made Arecibo suitable for Zeeman observations of the 21-cm line in the Galactic plane where the velocity gradients are very high. This is good news! With the upgraded Arecibo, we anticipate launching an energetic campaign to evaluate instrumental effects, derive methods for correcting them and observe magnetic fields.

Beam squint and other polarized sidelobes do not constitute the only instrumental difficulty. Bill Reach and I were trying to measure Zeeman splitting in a particular high-latitude cloud that he was studying in detail (G236+39; Reach, Koo and Heiles, 1994). We obtained a result that looked good. However, when we plotted the result versus hour angle the result changed sign near hour angle zero, where the azimuth arm swings most rapidly. We discovered this only "after the fact" and we presumed that it was related to tracking errors. Unfortunately, we did not have enough time to go back and investigate the details.

3. ZEEMAN SPLITTING POSSIBILITIES AT ARECIBO: A PERSONAL VIEW

3.1. Magnetic Fields in External Spiral Galaxies

The Galaxy is a sample of only one, and real understanding in astronomy comes from studying adequate samples. Magnetic fields in

some external galaxies exhibit bisymmetric structure or axisymmetric structure (e.g., M31; Beck, 1982), but most have no coherent structure (see Beck, 1993; Heiles, 1995a, b). These magnetic patterns are determined from Faraday rotation of their diffuse synchrotron radiation, which samples the Warm Ionized Medium (WIM)-weighted magnetic field as do pulsars in the Galaxy. However, Faraday rotation does not provide a truly representative view of the volume-averaged field in the Galaxy (Heiles, 1995b), so it is highly desirable to obtain independent observational information. Zeeman splitting of the 21-cm line radiation provides an excellent probe. In an edge-on external galaxy that is large enough to resolve, we can map the average field direction and strength along the major axis. This is roughly the equivalent of sampling the Galaxy along the "tangent points". To attain the necessary sensitivity we must use a filled aperture, which limits our resolution to the $\sim$3' attainable at Arecibo.

Four, and perhaps five, galaxies are good first choices for Arecibo. They include NGC3628, NGC4565, NGC4631, NGC5775, and NGC7331. The optical diameters of the first three exceed 12' and the HI diameters are much larger, so we can attain nearly ten pixels on these galaxies. The latter two are smaller. Other galaxies are too small to be mapped, but nevertheless we can obtain the integrated field sign and strength over each side of the disk because the two sides of the disk have opposite rotational Doppler shifts. For axisymmetric field configurations, the line-of-sight field in the major axis reverses at the galactic center, while for bisymmetric field configurations it does not. An observational study of a sample of unresolved edge-on galaxies will reveal the fraction of galaxies having these types of field patterns.

3.2. Zeeman Splitting of HI in Shocks and Filaments

Heiles (1989) measured Zeeman splitting of Galactic HI in nearby walls of shells (shocks) and filaments and found field amplification, as is expected for shocks on theoretical grounds. Supershells and worms exist over a large range of Galactocentric radius and the most prominent objects have been identified (Heiles, 1979; Heiles, 1984; Koo, Heiles and Reach, 1992; Heiles, Reach and Koo, 1996). Supershell and worm walls have swept up the gas and field from the

interiors and we believe that such swept-up, cool gas constitutes and important fraction of the Cold Neutral Medium (CNM; Heiles, 1982). The Arecibo telescope has the angular resolution required to isolate the gas in distant worm walls; the lines are fairly bright and the field strengths should be as easily detectable as those in nearer objects were with the HCRO 85-foot telescope. The distant objects may reflect the variation of field strength and direction with Galactocentric radius.

3.3. Direct Comparisons of Magnetic Fields in Molecular and Atomic Regions

The GBT, Arecibo and VLA telescopes are sensitive enough to see both HI and OH in absorption against the same continuum source in many cases. HI is the primary magnetic tracer for diffuse clouds and OH for dark clouds. Most of the HI in absorption towards a dark cloud should lie in the envelope of the dark cloud, while the OH lies further in. One expects the field inside clouds, measured by OH, to be larger than that outside, measured by HI. There are three sources for which measurements exist. Single-dish absorption results for Orion A (Troland, Crutcher and Kazés, 1986) and Orion B (Kazés and Crutcher 1986; van der Werf *et al.*, 1993) satisfy this expectation; Cas A (Heiles and Stevens, 1986) does not. However, single-dish results are not the whole story. VLA maps of HI in absorption against Orion A and Orion B, presented by Crutcher at this meeting, exhibit considerable angular structure in $B_{\|}$, with values reaching as high as 300 μG. This means that strict comparisons require high angular resolution. In addition, it may mean that the field strengths measured in HI and OH are comparable.

The continuum sources for this work must provide strong lines because even with Arecibo sensitivity will be an issue. The best source lists are in the original survey work for HI and OH absorption with single-dish telescopes – the classic papers – because any absorption line weak enough to require high sensitivity simply to detect it is too weak for Zeeman splitting measurements. In HI, one can select sources mainly from the classic list of Dickey, Salpeter and Terzian (1978); and in OH mainly from Goss (1968) and Dickey, Crovisier and Kazès (1981).

3.4. Magnetic Fields Near and in Dark Clouds with HI Self-Absorption and OH Emission

One of our first detections of HI Zeeman splitting was a "two-for-one" result: in a single profile, we had one detection in emission and another in self-absorption against Orion (Heiles and Troland 1982). This stimulated us to do more on HI self-absorption lines. In unpublished work with the HCRO 85-foot telescope, we attempted to survey the field strength in 47 dark clouds by measuring Zeeman splitting of the 21-cm line in self-absorption. This technique seemed promising because of the positive results we obtained in Ophiuchus (Goodman and Heiles, 1994) and in Taurus. We began with the catalog of self-absorption seen with the 140-foot telescope by Knapp (1974). Unfortunately, the larger beam size of the 85-foot telescope prevented us from seeing many of these self-absorption components. Most of those that we could see in self-absorption exhibited no detectable Zeeman splitting, but often an adjacent, narrow emission line component exhibited a detectable field. The well-known dark clouds L183 and L134 did exhibit fields detectable in self-absorption (3.3 and 5.0 μG, respectively).

Clearly, this survey needs to be repeated with a smaller beam size. Arecibo will be extremely useful for this work. It would be fascinating to employ Arecibo to examine self-absorption components along the Galactic plane, of which there are many (Bania and Lockman, 1984); this will not only increase the sample of clouds, but may also reveal the change in field strength with Galactocentric radius.

Our proposed survey of Zeeman splitting of HI self-absorption lines, which are strong and require relatively little telescope time, will generate a useful list of candidates for future OH Zeeman splitting observations with which to extend our comparisons of the field strengths in and near dark clouds. In Ophiuchus, the field strengths derived from Zeeman splitting of OH and HI are similar (Troland *et al.*, 1996), but not always identical in sign, which is surprising; clearly there is much to learn from these comparisons. Our final goal is to subject clouds to the detailed observational scrutiny and subsequent theoretical modelling in the manner of Crutcher *et al.* (1994).

3.5. Tiny-Scale Structure in the Cold Neutral Medium

Those astronomers who work on the neutral interstellar medium have become used to the idea, obtained from measurements of 21-cm emission lines, that the CNM has little structure below scales ~ 0.2 pc (Crovisier, Dickey and Kazès, 1985). However, at the same time one must recognize that smaller scale structure in the CNM does certainly exist: it is visible in optical photographs of HII regions and reflection nebulae (e.g., the dust filaments in the Pleiades), maps of the 21-cm line in absorption (e.g., Griesen and Liszt, 1986; Liszt, Dickey and Griesen, 1982), and studies of optical absorption lines against closely-spaced stars (Langer, Prosser and Sneden, 1990; Bates *et al.*, 1992). And, of course, in cold molecular gas there appears to be no small size scale threshold (e.g., Pound, Bania and Wilson, 1990; Marscher, Moore and Bania, 1993; Moore and Marscher, 1995).

There have been nagging indications from 21-cm line VLBI that tiny-scale structure exists in the CNM. Pioneered by Dieter, Welch and Romney (1976), Diamond *et al.* (1989) later observed 3C138, 3C147, and 3C380 and found tiny scale structure in all three, with the strongest in 3C138. Frail *et al.* (1994) also found such structure with a new technique, gaining high angular resolution by observing seven fast-moving pulsars over time. They conclude that tiny-scale structure in the CNM is common and contains a whopping 10% to 15% of the CNM. The changes in column density required to produce the observed time variations are $\delta N_{\rm HI} \sim 10^{20}\,{\rm cm}^{-2}$ and the length scales are ~ 30 A.U., implying volume densities for the tiny scale structure of $n_{\rm HI} \sim 10^5 (T/50\ {\rm K})\ {\rm cm}^{-3}$. This translates into a huge pressure, $P/k \sim 10^7 (T/50\ {\rm K})^2$, $\sim 10^3$ times the pressure usually adopted for the CNM, much larger than the pressure in any other gas component and far too large to be confined in the z direction under hydrostatic equilibrium (Boulares and Cox, 1990). Tiny-scale structure has also been seen in ionized gas with "Extreme Scattering Events" (ESE's; Fiedler *et al.*, 1994a); the implied column and volume densities are smaller but the pressures are comparable. There is no apparent correlation between the tiny-scale structure in neutral and ionized gas.

These observations can be no longer be ignored by those who study the "diffuse" ISM. We must confront the question of the origin and significance of such high densities and pressures. Column densities in

the ionized tiny-scale component are too small to study using traditional techniques such as RRL's. However, the neutral component has rather easily detectable column densities, particularly when one realizes that so far only the *change* in column density $\delta N_{\rm HI}$ has been observed; the *total* column densities should be larger.

We can imagine two physical processes that produce tiny-scale structure. One is fast shocks. ESE's are very rare and occur more frequently in sources near the major radio loops and nearby HI shells, and this perhaps suggests a shock origin (Fiedler *et al.*, 1994b). However, tiny-scale CNM is common and is neither correlated with ESE's nor has anomalous velocities (Frail *et al.*, 1994). Thus the origin of this high-density, high-pressure component of the CNM is puzzling. Cox (private communication) has suggested that this component may be confined by magnetic tension. If so, the magnetic field strengths must approach 100 μG. This is detectable. One might begin by using the Arecibo telescope to observe Zeeman splitting in the same HI absorption components found in the seven pulsars studied by Frail *et al.* (1994) and in 3C138, which was the strongest VLBI detection of Diamond *et al.* (1989).

3.6. Zeeman Splitting of Hydrogen Radio Recombination Lines: An Indirect Probe of Star-Forming Molecular Clouds

Arecibo will be equipped with correlation spectrometers that provide capability far beyond current devices. Hopefully, the Arecibo correlator will be able to measure eight Radio Recombination Lines (RRL's) at adjacent frequencies in the two polarizations simultaneously, thus multiplying the effective integration time. This makes it feasible to measure Zeeman splitting of any hydrogen RRL whose associated continuum brightness dominates the system temperature. The classic surveys (Reifenstein *et al.*, 1970; Downes *et al.*, 1980) provide the best source lists, and there are quite a few good first-look candidates.

The reader should immediately ask "Why bother?". There is nothing intrinsically interesting about the magnetic fields in HII regions because they occupy only a very small fraction of space and are special places. However, they should provide good indications of

the large-scale field strength of the parent molecular cloud within which the stars formed. The HII region gas was, before the star formation, part of the molecular cloud. When the gas became ionized its pressure increased by at least two orders of magnitude and should have totally dominated all other components, including magnetic pressure. The gas should have expanded roughly isotropically, with the magnetic field intact and $B \propto n_e^{-2/3}$. Other observational data provide good estimates of both n_e and also the density of the parent molecular cloud. Thus we can scale the field strength in the HII region to that in the parent cloud. One should also be able to fit the fields HII regions S117, S119, and S264, which were measured by Heiles, Chu and Troland (1981) using Faraday rotation, into this density-scaling scheme.

Using hydrogen RRL's and the density scaling argument is hardly an ideal technique, but there are very few probes of the large-scale field strength within molecular clouds. The only other successful probe of molecular clouds has been Zeeman splitting of OH. However, OH samples regions having a very large range in density, from $n(\mathrm{H_2}) \sim 10^4\,\mathrm{cm}^{-3}$down (see Heiles *et al.*, 1993; Troland *et al.*, 1996), and consequently biases results to the less dense outer portions of clouds.

3.7. Zeeman Splitting of Carbon Radio Recombination Lines: A Direct Probe of Star-Forming Molecular Clouds

Carbon RRL's sample dense photodissociation regions (PDR's), where the hydrogen is molecular but the carbon is singly ionized. Natta, Walmsley and Tielens (1994) find that the carbon RRL's in Orion come from very high density regions, $n_{\mathrm{H_2}} \sim 10^6\,\mathrm{cm}^{-3}$, with rather high temperatures, $T \sim 500 - 1000\,\mathrm{K}$; the pressures are enormous. In S140/L1204, where the carbon RRL is weaker, the densities are only $\sim 10^4\,\mathrm{cm}^{-3}$ (Smirnov, Sorochenko and Walmsley, 1995).

Zeeman splitting of the carbon RRL's offers a unique probe of the magnetic field in dense regions. In contrast to the hydrogen RRL's, the carbon RRL's sample the regions *directly*. The main impediment to measuring Zeeman splitting of carbon RRL's is the absence of a

sensitive, extensive survey of the carbon RRL's. From a possibly incomplete literature search, we find that the major survey is by Pankonin, Thomasson, and Barsuhn (1977), with supplementary work in the Arecibo declination range by Silverglate (1984a); line strengths seen with Arecibo are much larger than those with lesser telescopes! Nevertheless, all known lines are weak. We suspect that a new, extensive survey would uncover more regions with fairly strong lines.

As always, sensitivity is a real issue for Zeeman-splitting studies of these lines: Silverglate (1984b) attempted to detect Zeeman splitting of the carbon RRL in four regions and could only set upper limits at the ~ 1 mG level. The ability to observe many lines simultaneously, together with long integration times, will allow detection at the ~ 100 μG level. The potential scientific rewards are great because there are very few measurements or opportunities for measuring magnetic fields in dense star-forming regions.

3.8. Zeeman Splitting of the CH First Excited Rotational State: Another Direct Probe of Star-Forming Molecular Clouds

The first excited rotational state of CH ($^2\Pi_{3/2}$, $J = 3/2$) has four Λ-doubling transitions near 710 MHz that have high Landé-g factors (Heiles *et al.*, 1993). Ziurys and Turner (1985) used Arecibo to observe the two strongest of these transitions in absorption against the HII region W51 and found antenna temperatures ~ 0.5 K; they also saw the lines against the HII regions W3, W43 and Orion B. To excite the molecule to this state, collisions with H_2 are the only feasible mechanism and require $n(H_2) \sim 10^6\,\mathrm{cm}^{-3}$. This density is higher than that traced by any other molecule for which Zeeman splitting can realistically be measured (except in masers). Furthermore, all other molecular tracers for dense gas have mm-wavelength transitions, which makes their Zeeman splitting a much smaller fraction of the line width and consequently much harder to detect; the first effort on CN (Crutcher *et al.*, 1995) was unsuccessful and reached a limiting field strength of ~ 300 μG. In contrast, with this CH line at Arecibo one can rather easily see a field strength of 30 μG towards W51.

This means that one is almost assured of a positive detection. Generally, field strengths increase with density, roughly $\propto n^{1/2}$ (e.g.,

Troland 1989). Scaling from OH masers, which have $n(H_2) \sim 10^5$ to $10^5\,cm^{-3}$ and $B \sim 2 \times 10^3$ to 10^4 μG (Reid and Moran, 1981), one should find field strengths in the 10^2 to 10^3 μG range for the CH cloud in front of W51.

3.9. Zeeman Splitting of High-Redshift Absorption Systems

The physical processes that generate galactic magnetic fields are not well understood. There are two viewpoints: the fields are primordial (e.g., Kulsred and Anderson, 1992), and the fields are generated and regulated by dynamo mechanisms (e.g., Ferrière, 1993; Field, 1995). One way to distinguish between these two is to measure magnetic field strengths in high-redshift systems. Dynamo mechanisms on global galactic scales require cosmological time scales to build up the field, so fields should be weaker in high-redshift systems. Current evidence is based on Faraday rotation and suggests that field strengths near $Z \sim 2$ are too strong to have been generated by global galactic dynamos (Wolfe, Lanzetta and Oren, 1992; and Oren, 1992; Oren and Wolfe, 1995). However, the uncertainties are high because the Galactic Faraday rotation must be subtracted out.

One can bypass Faraday rotation by using Zeeman splitting to measure the field strengths. One would select damped Lyα systems, in which a high-Z spiral galaxy lies in front of a more distant quasar and its CNM gives rise to strong, fairly narrow 21-cm line absorption. There are three good candidates with relatively strong lines for which we can easily detect fields at the 3 μG level at Arecibo. These systems include 0235+164 with $Z \sim 0.52$ (Roberts *et al.*, 1976), 0458-02 with $Z \sim 2.04$ (Wolfe *et al.*, 1985), and 1328+327 (3C286) with $Z \sim 0.39$ (Brown and Roberts, 1973).

By far the most interesting source is PKS0458-02 because it has a strong, narrow line and the largest redshift. At 465 MHz, though, there is a problem: interference. And at declination -2°, there is another problem: it is outside the nominal declination range for Arecibo. As time goes on the interference environment gets worse, and for this reason alone we cannot wait for precession to bring the source into the nominal declination range! So we throw down the gauntlet and state two real challenges for Arecibo Observatory:

(1) Can Arecibo overcome the interference, for example by using as-yet uninvented interference suppression techniques or by locating the interference-producing transmitters and persuading them to cooperate for a few weeks?
(2) Arecibo has a tradition of "can-do". Once it somehow managed to observe the source at declination $-2°$. Does it still continue this tradition?

4. CONCLUSION: ARECIBO AND ZEEMAN SPLITTING

Magnetic fields are interesting because they are strong enough to drastically affect physical processes in the interstellar medium. However, they are difficult to measure because they require high sensitivity and attention to instrumental problems. The instrumental problems are difficult but hardly impossible to solve; in particular, Arecibo's predicted beam squint of $\lesssim 0.3'$ is small enough to neglect for many situations, and first-order corrections should safely remove the beam-squint instrumental contribution for the rest. As recounted above in 2.5, beam squint is not the only problem. Zeeman splitting studies of emission lines are fraught with instrumental effects that have to be handled with great care.

Magnetic fields are one of the dominant forces on most forms of interstellar gas. Arecibo offers many interesting possibilities for measurements of Zeeman splitting, and I have covered a few of them here. More will be discussed by Crutcher in the next paper. Measuring magnetic fields can ocupy Arecibo full time for the next few decades!

References

Bania, T. M. and Lockman, F. J. (1984) *ApJ Suppl.*, **54**, 513.
Bates, B., Wood, K. D., Catney, M. G. and Gilheany, S. (1992) *MNRAS*, **254**, 221.
Beck, R. (1982) *A&A*, **106**, 121.
Beck, R. (1993) in The Cosmic Dynamo, IAU Symp. No. 157, F. Krause, K.-H. Rädler and G. Rüdiger, Dordrecht: Kluwer, 283.
Boulares, A. and Cox, D. P. (1990) *ApJ*, **365**, 544.
Brown, R. L. and Roberts, M. S. (1973) *ApJ*, **184**, L7.
Crovisier, J., Dickey, J. M. and Kazés, A. (1985) *A&A*, **146**, 223.
Crutcher, R. M., Kazés, I. and Troland, T. H. (1987) *A&A*, **181**, 119.
Crutcher, R. M., Mouschovias, T. Ch., Troland, T. H. and Ciolek, G. E. (1994) *ApJ*, **427**, 839.

Crutcher, R. M., Troland, T. H., Lazereff, B. and Kazés, I. (1995) *ApJ*, **000**, L000.
Diamond, P. J., Goss, W. M., Romney, J. D., Booth, R. S., Kalberla, P. M. W. and Mebold, U. (1989) *ApJ*, **347**, 302.
Dickey, J. M., Crovisier, J. and Kazès, I. (1981) *A&A*, **98**, 271.
Dickey, J. M., Salpeter, E. E. and Terzian, Y. (1978) *ApJSuppl.*, **36**, 77.
Dieter, N. H., Welch, W. J. and Romney, J. D. (1976) *ApJ*, **206**, L113.
Downes, D., Wilson, T. L., Bieing, J. and Wink, J. (1980) *A&A Suppl.*, **40**, 379.
Ferrière, K. (1993) *ApJ*, **409**, 248.
Fiedler, R., Dennison, B., Johnston, K. J., Waltman, E. B. and Simonk, R. S. (1994a) *ApJ*, **430**, 581.
Fiedler, R., Pauls, T., Johnston, K. J. and Dennison, B. (1994b) *ApJ*, **430**, 595.
Field, G. B. (1995) in *The Physics of the Interstellar Medium and Intergalactic Medium*, ASP Conference Series **80**, ed. A. Ferrara, C. F. McKee, C. Heiles and P. R. Shapiro, p. 1.
Frail, D. A., Weisberg, J. M., Cordes, J. M. and Mathers, C. (1994) *ApJ*, **436**, 144.
Goodman, A. A., Crutcher, R. M., Heiles, C., Myers, P. C. and Troland, T. H. (1989) *ApJ*, **338**, L61.
Goodman, A. A. and Heiles, C. (1994) *ApJ*, **424**, 208.
Goss, W. M. (1968) *ApJ Suppl*, **15**, 131.
Greisen, E. W. and Liszt, H. S. (1986) *ApJ*, **303**, 702.
Heiles, C. (1979) *ApJ*, **229**, 533.
Heiles, C. (1982) *ApJ*, **262**, 135.
Heiles, C. (1984) *ApJ Suppl.*, **55**, 585.
Heiles, C. (1989) *ApJ*, **336**, 808.
Heiles, C. (1990) in *Galactic and Intergalactic Magnetic Fields*, IAU Symposium No. 140, Ed. Beck, R. *et al.*, p. 35.
Heiles, C. (1995a) in *The Physics of the Interstellar and Intergalactic Medium*, ASP Conference Series Volume 80, ed. A. Ferrara, C. F. McKee, C. Heiles and P. R. Shapiro, p. 507.
Heiles, C. (1995b) in *Polarimetry of the Interstellar Medium*, ASP Conference Series Volume 000, Ed. W. G. Roberge and D. C. B. Whittet.
Heiles, C. (1996) *ApJ*, submitted.
Heiles, C., Chu, Y.-H. and Troland, T. H. (1981) *ApJ*, **247**, L77.
Heiles, C., Goodman, A. A., McKee, C. and Zweibel, E. (1993) in *Protostars and Planets III*, ed. E. H. Levy and J. I. Lunine, University of Arizona Press: Tucson, p. 279.
Heiles, C., Reach, W. T. and Koo, B.-C. (1996) *ApJ*, submitted.
Heiles, C. and Stevens, M. (1986) *ApJ*, **301**, 331.
Heiles, C. and Troland, T. H. (1982) *ApJ*, **260**, L23.
Heithausen, A. and Thaddeus, P. (1990) *ApJ*, **353**, 149.
Kazés, I. and Crutcher, R. M. (1986) *A&A*, **164**, 328.
Knapp, G. R. (1974) *AJ*, **79**, 527.
Koo, B.-C., Heiles, C. and Reach, W. T. (1992) *ApJ*, **390**, 108.
Kulsred, R. M. and Anderson, S. W. (1992) *ApJ*, **396**, 606.
Langer, G. E., Prosser, C. F. and Snedon, C. I. (1990) *ApJ*, **100**, 216.
Liszt, H. S., Dickey, J. M. and Griesen, E. W. (1982) *ApJ*, **261**, 102.
Marscher, A. P., Moore, E. M. and Bania, T. M. (1993) *ApJ*, **419**, L101.
Moore, E. L. and Marscher, A. P. (1995) *ApJ*, **452**, 671.
Natta, A., Walmsley, C. M. and Tielens, A. G. G. M. (1994) *ApJ*, **428**, 209.
Oren, A. L. and Wolfe, A. M. (1995) *ApJ*, **445**, 624.
Pankonin, V., Thomasson, P. and Barsuhn, J. (1977) *A&A*, **54**, 335.
Pound, M. W., Bania, T. M. and Wilson, R. W. (1990) *ApJ*, **351**, 165.
Reach, W. T., Koo, B.-C. and Heilies, C. (1994) *ApJ*, **429**, 672.
Reid, M. J. and Moran, J. M. (1981) *ARAA*, **19**, 231.

Reifenstein, E. C., Wilson, T. L., Burke, B. F., Meger, P. G. and Altenhoff, W. J. (1970) *A&A*, **4**, 357.
Roberts, M. S., Brown, R. L., Brundage, W. D., Rots, A. H., Haynes, M. P. and Wolfe, A. M. (1976) *AJ*, **82**, 193.
Silverglate, P. R. (1984a) *ApJ*, **278**, 604.
Silverglate, P. R. (1984b) *ApJ*, **279**, 694.
Smirnow, G. T., Sorochenko, R. L. and Walmsley, C. M. (1995) *A&A*, **300**, 923.
Troland, T. H. (1989) in *Galactic and Intergalactic Magnetic Fields*, IAU Symposium 140, Ed. R. Beck, P. P. Kronberg and R. Wielebinski p. 293.
Troland, T. H., Crutcher, R. M. and Kazés, I. (1986) *ApJ*, **304**, L57.
Troland, T. H., Crutcher, R. M., Goodman, A. A., Heiles, C., Kazès, I. and Myers, P. C. (1996) *ApJ*, to be submitted.
Troland, T. H. and Heiles, C. (1982) *ApJ*, **252**, 179 (TH).
van der Werf, P. P., Goss, W. M., Heiles, C., Crutcher, R. and Troland, T. H. (1993) *ApJ*, **411**, 247.
Verschuur, G. L. (1969) *ApJ*, **156**, 861.
Verschuur, G. L. (1989) *ApJ*, **339**, 163.
Verschuur, G. L. (1993) *BAAS*, **25**, 1466.
Verschuur, G. L. (1995a) *ApJ*, **451**, 624.
Verschuur, G. L. (1995b) *ApJ*, **451**, 645.
Wolfe, A. M., Briggs, F. H., Turnshek, D. A., Davis, M. M., Smith, H. E. and Cohen, R. D. (1985) *ApJ*, **294**, L67.
Wolfe, A. M., Lanzetta, K. M. and Oren, A. L. (1992) *ApJ*, **388**, 17.
Ziurys, L. M. and Turner, B. E. (1985) *ApJ*, **292**, L25.